RESEARCH ARTICLE | OCTOBER 31 2007

Series resistance imaging of solar cells by voltage dependent electroluminescence

David Hinken; Klaus Ramspeck; Karsten Bothe; Bernhard Fischer; Rolf Brendel

Appl. Phys. Lett. 91, 182104 (2007)
https://doi.org/10.1063/1.2804562

Series resistance imaging of solar cells by voltage dependent electroluminescence

David Hinken,[a] Klaus Ramspeck, Karsten Bothe, Bernhard Fischer, and Rolf Brendel
Institut für Solarenergieforschung Hameln/Emmerthal (ISFH), Am Ohrberg 1, 31860 Emmerthal, Germany

(Received 27 August 2007; accepted 10 October 2007; published online 31 October 2007)

This letter introduces a method based on electroluminescence imaging to determine mappings of the local series resistance of large area semiconductor devices such as solar cells. The method combines the local electroluminescence emission $\Phi_i(U)$ and its derivative $\Phi_i'(U)$ with respect to the applied voltage U. The combined analysis of these two quantities yields the local series resistance R_i^{se} and proves the physical validity of the used current transport model and thus the physical relevance of the determined R_i^{se} value. The method is verified on a monocrystalline silicon solar cell with local shunts and local series resistance problems. © *2007 American Institute of Physics*.
[DOI: 10.1063/1.2804562]

For high current devices, such as solar cells, minimizing ohmic series resistance losses is of vital importance. The analysis of the series resistance (R^{se}) not only requires an accurate determined value but should also give a conclusive proof of its correctness. A numerical agreement between the measured and simulated current-voltage (*I-V*) curves is not sufficient.[1] Thus, Werner[1] proposed a method that not only is based on the analysis of measured *I-V* curves but also takes into account the slope of these curves. The combined analysis of these two quantities directly shows the validity of the underlying current transport model and thus allows proving of the correctness of the calculated R^{se} value.

Solar cells are large area devices which require a high lateral conductivity. Limitations in the conductivity of the finger grid and a nonvanishing emitter sheet resistance result in local variations of the series resistance. Thus, a lumped series resistance is only of limited benefit when seeking the origin of a locally increased R^{se} value.

Various techniques have been developed to determine mappings of the local series resistance of solar cells. Scanning techniques are contact resistance scanning,[2] where the local potential is probed under local illumination, and solar cell local characterization,[3] which is based on the light beam induced current[4] (LBIC) technique.

Recently, camera based techniques have been introduced. Qualitative images of the series resistance distribution have been achieved using lock-in thermography.[5,6] Two quantitative methods for the local series resistance determination have been demonstrated using luminescence imaging.[7,8] Trupke *et al.*[7] calculated the local R^{se} values from photoluminescence images captured at two working points, while Ramspeck *et al.*[8] combined electroluminescence[9] (EL) and dark lock-in thermography[10] (DLIT) images.

So far, no method has been introduced which determines the local R_i^{se} values and verifies the validity of the model used for the current transport. Therefore, in this work, we use the approach of Werner for the analysis of electroluminescence images captured at different applied voltages using a silicon charge-coupled device (CCD) camera. The local series resistance R_i^{se} follows from the evaluation of the local electroluminescence signal Φ_i and its derivative Φ_i' with respect to the applied voltage U. A deviation from the expected linear behavior in Φ'/Φ vs Φ' curves reveals the failure of the model used for the current transport.

The experimental setup comprises a cooled silicon CCD gray scale camera mounted in a dark box. Each pixel of the camera collects for a 12.5×12.5 cm^2 solar cell the luminescence emission Φ_i of a 120×120 μm^2 area at the position i. Using a four-point contacting scheme, a bipolar power supply regulates the applied voltage U and the external current I of the solar cell. During the measurements, a thermostat stabilizes the temperature of the solar cell at 25 °C.

To obtain the EL signal Φ_i as well as its derivative Φ_i' with respect to the applied voltage U, we modulate U with a small voltage ΔU in a three step signal, $U+\Delta U/2$ (step 1), $U-\Delta U/2$ (step 2), and 0 (step 3). During each step, the camera takes an image with equal exposure time. The electroluminescence image Φ follows as the average of the images of steps 1 and 2. The subtraction of the dark image taken in step 3 removes artificial signals such as stray light and dark signal. The differential electroluminescence image $\Delta\Phi$ is the difference of the images of steps 1 and 2. Artificial signals are removed in this difference image automatically as they are contained in both original images. Dividing each pixel of the image $\Delta\Phi$ by ΔU results in the derivative $\Phi_i'(U)=\Delta\Phi_i/\Delta U$.

In order to correct the images Φ and $\Delta\Phi$ for lateral inhomogeneities of the objective transmittance as well as for different pixel sensitivities of the CCD chip, we divide them by a calibration image of a homogeneous luminescence light source. We average multiple images taken at the same voltage to improve the signal-to-noise ratio (SNR). The measurement of $\Phi'(U)$ requires a ΔU as small as possible. However, a good SNR is obtained with a high $\Delta\Phi$ signal and thus a high ΔU. As a compromise, we use $\Delta U=10$ mV or $U\leqslant600$ mV and $\Delta U=5$ mV for $U>600$ mV.

The local luminescence emission per second relates to the local voltage U_i by[11]

[a]Electronic mail: hinken@isfh.de

$$\Phi_i = C_i \exp(U_i/U_T). \quad (1)$$

Here, $U_T = k_B T/q$ is the thermal voltage and C_i a calibration constant containing material and optical properties of the sample and the setup.

For our considerations, we model the solar cell by a two-dimensional parallel network of equivalent circuits. We describe each circuit i by a one-diode model which consists of a local shunt resistance R_i^{sh}, a local diode with a dark saturation current J_{0i}, and a local series resistance R_i^{se}. R_i^{se} represents the resistance along the current path from the position i of the solar cell to the contacts and therefore includes contributions from the emitter, contact, and finger resistances.

In each circuit i, the sum of the voltage U_i at the diode and the voltage drop ΔU_i at the series resistance gives the applied voltage U:

$$U = U_i + \Delta U_i. \quad (2)$$

We calculate U_i by rearranging Eq. (1) and ΔU_i using Ohm's law with the current densities J_i and U_i/R_i^{sh} through the local diode and the local shunt, respectively,

$$U_i = U_T \ln(\Phi_i/C_i), \quad (3)$$

$$\Delta U_i = R_i^{se}(J_i + U_i/R_i^{sh}). \quad (4)$$

We describe the local diode by $J_i = J_{0i} \exp(U_i/U_T)$ with an ideality factor of $n=1$ and assume J_{0i} to be injection independent. The combination of this equation with Eq. (3) yields J_i

$$J_i = \Phi_i J_{0i}/C_i. \quad (5)$$

Replacing U_i and ΔU_i in Eq. (2) leads to

$$U = U_T(1 + R_i^{se}/R_i^{sh})\ln(\Phi_i/C_i) + \Phi_i R_i^{se} J_{0i}/C_i. \quad (6)$$

The latter equation implicitly describes the impact of shunt and series resistances on the local luminescence emission at an applied voltage U.

To determine R_i^{se}, we use a data evaluation procedure in analogy to the approach of Werner and differentiate Eq. (6) with respect to U:

$$U_T \Phi_i'/\Phi_i = b - b\Phi_i' R_i^{se} J_{0i}/C_i, \quad (7)$$

with $1/b = 1 + R_i^{se}/R_i^{sh}$ and $\Phi_i' = \Delta\Phi_i/\Delta U$ which is measured as explained above. According to Eq. (7), data points are expected to lie on a straight line in a $U_T\Phi'/\Phi$ vs Φ' plot. By means of curve fitting, we determine the slope m and the intercept b. The local series resistance is then given by

$$R_i^{se} = -\frac{C_i}{J_{0i}}\frac{m}{b}. \quad (8)$$

To determine the scaling factor C_i/J_{0i}, we sum up Eq. (5) over the whole cell area $\Sigma J_i = \Sigma \Phi_i J_{0i}/C_i$. ΣJ_i is replaced by I/A, where A is the solar cell area imaged by a pixel, since the external current I is the sum of all local currents. J_{0i}/C_i is assumed to be laterally homogeneous and thus independent of i. We therefore end up with

$$C_i/J_{0i} = \frac{\sum \Phi_i}{I/A}. \quad (9)$$

Each deviation from a straight line in a $U_T\Phi'/\Phi$ vs Φ' plot reveals a failure of the used current transport model and implies that the corresponding R_i^{se} value is incorrect.

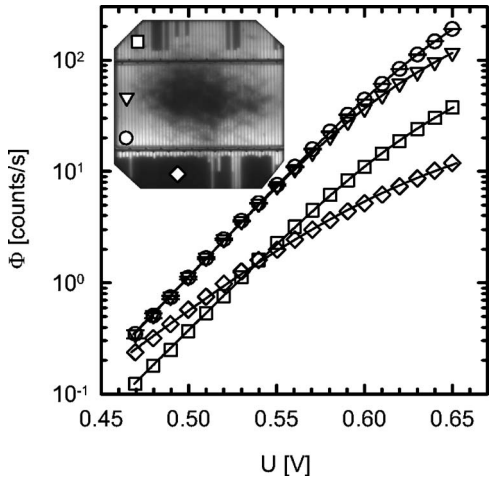

FIG. 1. Voltage dependent local electroluminescence emission from regions limited by shunts or series resistances. The solid lines represent the fits of the data using Eq. (6). Circles and triangles: well contacted regions close to a bus bar and in between the bus bars, respectively; squares: region with a shunt; diamonds: poorly contacted region due to many disconnected fingers; small inlet: electroluminescence image captured at 650 mV illustrating the positions of the analyzed regions.

We demonstrate the data evaluation procedure on a monocrystalline solar cell with local shunts (verified with DLIT) and local series resistance problems and take Φ and Φ' image pairs with applied forward voltages ranging from 470 to 650 mV.

Figure 1 shows resulting $\Phi_i(U)$ curves and illustrates the positions of the analyzed regions in an inset. The $\Phi_i(U)$ curves of well (circles, triangles) and poorly (diamonds) contacted regions converge for low applied forward voltages since series resistance effects become negligible due to the small current flow. In contrast, at higher applied voltages, the impact of a series resistance leads to a decreasing slope compared to the ideal exponential behavior of Eq. (1). Even though the $\Phi_i(U)$ curve of the region with a shunt (squares) has a similar shape compared to the well contacted regions (circles, triangles), it is shifted to lower Φ values. The high current flow through the shunt path even at low voltages leads to a voltage drop at the series resistance which consequently results in a reduced Φ signal.

Figure 2 shows the Φ'/Φ vs Φ' plot for the same data as in Fig. 1. To ensure readability, we give error bars for the well contacted region only (circles) and omit data points below $U=540$ mV. Thus, in each curve, the leftmost data point correlates to 540 mV and the rightmost to 650 mV, since a high Φ' indicates a high external voltage. All data points in Fig. 2 (except diamonds) lie on a straight line, cutting the axis of the ordinate just below unity, as expected from Eq. (7). The observed linearity over the whole voltage range justifies the underlying current transport model and the local series resistance can be determined correctly. The resulting values are shown in Fig. 2. The poorly contacted region (diamonds) shows a significant deviation from the expected linear behavior. For this region, the local series resistance is limited by the distributed emitter sheet resistance which cannot be explained by the used current transport model. However, this investigation is beyond the scope of this paper and will be discussed in a further publication. The ordinate b of the linear fit to the measured data for the region with a shunt

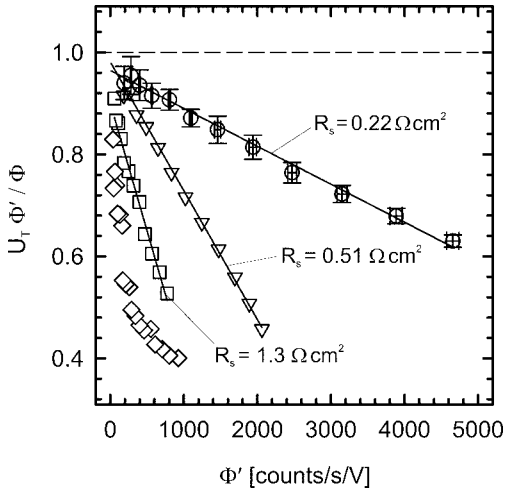

FIG. 2. The same data as in Fig. 1 in a Φ'/Φ vs Φ' plot. The slope and the intercept of a linear fit (solid lines) yield the local series resistance value. Note: To ensure readability, for the data shown as diamonds, the x coordinate is multiplied by a factor of 5.

(squares) is 0.90 and that for the well contacted regions (circles and triangles) is >0.95, suggesting a criterion for an automated shunt detection.

Figure 3(a) shows an image of the local series resistance obtained by applying the introduced method to all pixels. Locally, we determine very high series resistances (>5 $\Omega\,cm^2$) caused by disconnected fingers (top and bottom regions) and contact resistances (centered region). The left and the right side show typical local series resistances between 0.2 and 0.5 $\Omega\,cm^2$. Here, we observe the increase in R_i^{se} with rising distance to the bus bars and in between the fingers due to the finger resistance and the emitter sheet resistance, respectively, demonstrating the high accuracy for low series resistances and the high spatial resolution. For comparison, Fig. 3(b) shows a series resistance image in the same logarithmic scale using the recombination current and series resistance imaging (RESI) approach by Ramspeck *et al.*[8] For the regions next to and in between the bus bars, RESI yields values of 0.21 $\Omega\,cm^2$ (circle) and 0.48 $\Omega\,cm^2$ (triangle), which are in very good agreement to the method introduced in this letter (see values given in Fig. 2). Due to the observed nonlinearity of the poorly contacted region

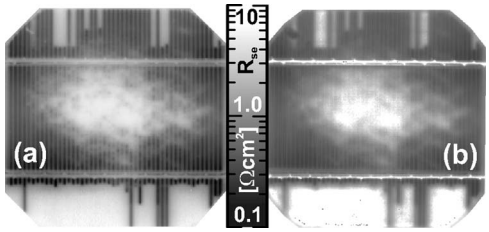

FIG. 3. Series resistance image obtained by the method introduced in this letter (a) and for comparison using the RESI (Ref. 8) approach (b). Both images use a logarithmic scale from 0.1 to 10 $\Omega\,cm^2$.

(diamonds in Fig. 2), the resulting series resistance value is not well determined and neither agrees with the RESI method.

For the calculation of the local series resistance, we assumed that the solar cell can be modeled as a network of equivalent circuits, whereas each circuit is described independently by a one-diode model. The real solar cell is far more complex, thus, it is important to check the physical relevance of the determined R_i^{se} value by a linear behavior in the Φ'/Φ vs Φ' plot. For a simple and fast local R_i^{se} characterization, a single Φ and Φ' image pair is sufficient, keeping the solar cell at one working point. The assumption of a lateral homogeneous scaling factor J_{0i}/C_i is valid as long as lateral variations in the effective bulk lifetime and the optical properties of the cell are negligible. It is a good assumption for monocrystalline cells but leads to errors for multicrystalline material. The latter restriction can be surmounted by determining J_{0i} from spectrally resolved LBIC measurements and C_i from an EL image captured under low applied voltage.

In this letter, we presented a method to obtain mappings of the local series resistance based on the combined analysis of the local electroluminescence signal Φ_i and its derivative Φ_i' with respect to the applied voltage. The procedure not only determines values for the local series resistance but also confirms the validity of the underlying current transport model and thus proves the physical relevance of the determined value. Applied to large area solar cells, we obtained a high resolution series resistance image, in good agreement to the recently introduced RESI method.

This work was funded by the Federal Ministry for the Environment, Nature Conservation, and Nuclear Safety under Contract No. 0327661.

[1] J. Werner, Appl. Phys. A: Solids Surf. **47**, 291 (1988).
[2] A. van der Heide, J. Bultman, J. Hoornstra, and A. Schönecker, Sol. Energy Mater. Sol. Cells **74**, 43 (2002).
[3] J. Carstensen, G. Popkirov, J. Bahr, and H. Föll, Sol. Energy Mater. Sol. Cells **76**, 599 (2003).
[4] W. Warta, J. Sutter, B. Wagner, and R. Schindler, in *Proceedings of the Second World Conference and Exhibition on Photovoltaic Solar Energy Conversion, Vienna, Austria, 1998* (EC Joint Research Center, Ispra, 1998), p. 1650.
[5] J. Isenberg, A. van der Heide, and W. Warta, Prog. Photovoltaics **13**, 697 (2005).
[6] O. Breitenstein and J. Rakotoniaina, J. Appl. Phys. **97**, 074905 (2005).
[7] T. Trupke, E. Pink, R. Bardos, and M. Abbott, Appl. Phys. Lett. **90**, 093506 (2007).
[8] K. Ramspeck, K. Bothe, D. Hinken, B. Fischer, J. Schmidt, and R. Brendel, Appl. Phys. Lett. **90**, 153502 (2007).
[9] T. Fuyuki, H. Kondo, T. Yamazaki, Y. Takahashi, and Y. Uraoka, Appl. Phys. Lett. **86**, 262108 (2005).
[10] O. Breitenstein and M. Langenkamp, *Lock-in Thermography* (Springer, Berlin, 2003), Vol. 10.
[11] K. Bothe, P. Pohl, J. Schmidt, T. Weber, P. Altermatt, B. Fischer, and R. Brendel, in *Proceedings of the 21st European Photovoltaic Solar Energy Conference, Dresden, Germany, 2006* (WIP, Munich, 2006), p. 597.